European Journal of Pharmacology 588 (2008) 259–266

Contents lists available at ScienceDirect

European Journal of Pharmacology

journal homepage: www.elsevier.com/locate/ejphar

Amyloid beta peptide-activated signal pathways in human platelets

Ming Y. Shen [a], George Hsiao [a], Tsorng H. Fong [b], Hui M. Chen [b], Duen S. Chou [a], Chien H. Lin [a,c], Joen R. Sheu [a,c,*], Chung Y. Hsu [c,d,e]

[a] Graduate Institute of Medical Sciences, College of Medicine, Taipei Medical University, Taipei, Taiwan
[b] Department of Anatomy, Taipei Medical University, Taipei, Taiwan
[c] Topnotch Stroke Research Center, Taipei Medical University, Taipei, Taiwan
[d] Department of Neurology, Taipei Medical University, Taipei, Taiwan
[e] Chi-Chin Huang Stroke Research Center, Taipei Medical University, Taipei, Taiwan

ARTICLE INFO

Article history:
Received 13 November 2007
Received in revised form 4 March 2008
Accepted 9 April 2008
Available online 22 April 2008

Keywords:
Amyloid-β
PAR1
Platelet
p38 MAPK
PI3-kinase/Akt

ABSTRACT

Amyloid beta peptide (amyloid-β), which accumulates in the cerebral microvessels in an age-dependent manner, plays a key role in the pathogenesis of cerebral amyloid angiopathy. Platelets are an important cellular element in vasculopathy of various causes. Amyloid-β may activate or potentiate platelet aggregation. The present study explored the signaling events that underlie amyloid-β activation of platelet aggregation. Platelet aggregometry, immunoblotting and assays to detect activated cellular events were applied to examine the signaling processes of amyloid-β activation of platelets. Exogenous amyloid-β (1–2 μM) potentiated platelet aggregation caused by collagen and other agonists. At higher concentrations (5–10 μM), amyloid-β induced platelet aggregation which was accompanied by an increase in thromboxane A_2 (TxA_2) formation. These amyloid-β actions on platelets were causally related to amyloid-β activation of p38 mitogen-activated protein kinase (MAPK). Inhibitors of p38 MAPK and its upstream signaling pathways including proteinase-activated receptor 1 (PAR1), Ras, phosphoinositide 3-kinase (PI3-kinase), or Akt, but not extracellular signal-regulated kinase 2 (ERK2)/c-Jun N-terminal kinase 1 (JNK1), blocked amyloid-β-induced platelet activation. These findings suggest that the p38 MAPK, but not ERK2 or JNK1 pathway, is specifically activated in amyloid-β-induced platelet aggregation with the following signaling pathway: PAR1 → Ras/Raf → PI3-kinase → Akt → p38 MAPK → cytosolic phospholipase A_2 ($cPLA_2$)→ TxA_2. In conclusion, this study demonstrates amyloid-β activation of a p38 MAPK signaling pathway in platelets leading to aggregation. Further studies are needed to define the specific role of amyloid-β activation of platelets in the pathogenesis of vasculopathy including cerebral amyloid angiopathy.

1. Introduction

Amyloid-β peptide, a major mediator of neuronal death, is also cytotoxic to cerebral endothelial cells and vascular smooth muscle cells and has been implicated in the pathogenesis of cerebral amyloid angiopathy (Herzig et al., 2004; Fryer et al., 2005; Zhang-Nunes et al., 2006; Hsu et al., 2007). Amyloid-β containing 39~43 amino acid residues is derived from the proteolytic cleavage of amyloid precursor protein (APP). The major amyloid-β species found in vascular plaques is amyloid-β_{1-40}, while the dominant species in neuronal plaques is amyloid-β_{1-42} (Herzig et al., 2004; Fryer et al., 2005). The cellular sources of amyloid-β deposited in neuronal or vascular plaques remain to be delineated. Soluble amyloid-β probably originates from cells within the central nervous system as well as the peripheral circulation (Wisniewski et al., 1997; Mackic et al., 2002; Tedgui and Mallat, 2002; van Dijk et al., 2004; Gurol et al., 2006).

Indeed, human platelets contain high levels of APP, which may contribute to more than 90% of the circulating APP (Li et al., 1994). Platelet APP may also be the major source of amyloid-β detected in whole blood (Chen et al., 1995). Aβ is released upon platelet activation (Smith, 1997). The main species of amyloid-β released from activated human platelets is amyloid-β_{1-40}, consistent with the contention that circulating amyloid-β contributes to vascular amyloid deposits dominated by amyloid-β_{1-40} (Skovronsky et al., 2001; Herzig et al., 2004; Fryer et al., 2005). It is interesting to note that misfolding amyloid-β is capable of inducing platelet aggregation (Herczenik et al., 2007). This finding raises the possibility that amyloid-β activation of platelets may set a vicious cycle in platelet activation and release of amyloid-β. However, the more detailed mechanisms by which amyloid-β activated platelets remains to be defined. In this study, we systematically examined the cellular events associated with amyloid-β-induced platelet activation in vitro, and utilized the findings to characterize the mechanisms involved in this influence.

* Corresponding author. Graduate Institute of Medical Sciences, College of Medicine, Taipei Medical University, 250 Wu-Hsing Street, Taipei 110, Taiwan. Tel.: +886 2 27361661 3199; fax: +886 2 27390450.
E-mail address: sheujr@tmu.edu.tw (J.R. Sheu).

0014-2999/$ – see front matter © 2008 Elsevier B.V. All rights reserved.
doi:10.1016/j.ejphar.2008.04.040

2. Materials and methods

2.1. Materials

Amyloid-β (Amyloid-β_{25-35} and Amyloid-β_{1-40}), collagen (type I, bovine Achilles tendon), prostaglandin E_1 (PGE_1), bovine serum albumin (BSA), dimethyl sulfoxide (DMSO), heparin, manumycin A, adenosine 5′-diphosphate (ADP), arachidonic acid, aristolochic acid, and thrombin were purchased from Sigma Chem. (St Louis, MO); *N*-3-cyclopropyl-7-{[4-(1-methyl-ethyl)phenyl]methyl}-7H-pyrrolo[3,2-f] quinazoline-1,3-diamine (SCH79797) from TOCRIS Bioscience (Ellisville, MO); *trans*-cinnamoyl-YPGKF-NH2 from Peptides International Inc. (Louisville, KY); Fura 2-AM from Molecular Probe (Eugene, OR); the thromboxane B_2 enzyme immunoassay (EIA) kit from Cayman (Ann Arbor, MI); anti-phospho-p38 MAPK (Ser^{182}) monoclonal antibody (mAb), 2′-amino-3′-methoxyflavone (PD98059) and 4-[5-(4-Fluorphenyl)-2-[4-(methylsulfonyl) phenyl]-1H-imidazol-4-yl] pyridine (SB203580) from Santa Cruz (Santa Cruz, CA); 2-(4-morpholino)-8-phenyl-4H-1-benzopyran-4-one (LY294002) and anthra [1-9cd] pyrazol-6(2H)-one (SP600125) from Calbiochem (San Diego, CA); anti-p38 mitogen-activated protein kinase (MAPK), anti-phospho-SAPK/JNK (Thr^{183}/Tyr^{185}), anti-phospho-p44/p42 extracellular signal-regulated kinase (ERK) (Thr^{202}/Tyr^{204}) and anti-p44/p42 ERK pAb from Cell Signaling (Beverly, MA); anti-phospho-Akt (Ser^{473}), anti-Akt, anti-c-Jun N-terminal kinase 1 (JNK1) polyclonal antibody (pAbs) and Akt-I from Biovision (Mountain View, CA); the Ras activation assay kit from Upstate Biotech. (Temecula, CA); the Hybond-P PVDF membrane, ECL Western blotting detection reagent and analysis system, horseradish peroxidase-conjugated donkey anti-rabbit IgG, and sheep anti-mouse IgG from Amersham (Buckinghamshire, UK).

2.2. Platelet aggregation

Human platelet suspensions were prepared as previously described (Hsiao et al., 2005). This study conformed to the principles outlined in the *Helsinki Declaration*, and human volunteers gave informed consent. In brief, blood was collected from healthy human volunteers who had taken no medicine during the preceding 2 weeks, and mixed with acid/citrate/glucose (9:1, v/v). After centrifugation 120 ×*g*, the supernatant (platelet-rich plasma) was supplemented with prostaglandin E_1 (PGE_1; 0.5 μM) and heparin (6.4 IU/ml) and then centrifuged at 500 ×*g*. The washed platelets were finally suspended in Tyrode's solution. Platelet suspensions (3.6×10^8 platelets/ml, 0.4 ml) were pretreated with or without reagents for 3 min, followed by the addition of amyloid-β or other agonists. The reaction was allowed to proceed for at least 6 min, and the extent of aggregation was expressed in light-transmission units.

2.3. Measurement of platelet $[Ca^{+2}]i$ mobilization by Fura 2-AM fluorescence

Assessment of platelet $[Ca^{+2}]i$ mobilization based on Fura 2-AM fluorescence has been reported (Hsiao et al., 2005). Briefly, citrated platelet-rich plasma was incubated with Fura 2-AM (5 μM) for 1 h. Fura 2-AM-loaded platelets were isolated and then suspended in Tyrode's solution. $[Ca^{+2}]i$ was monitored using a fluorescence spectrophotometer (CAF 110, Jasco, Tokyo, Japan) at excitation wavelengths of 340 and 380 nm and an emission wavelength of 500 nm.

2.4. Measurement of thromboxane B_2 formation

As described previously (Sheu et al., 1999; Hsiao et al., 2007), washed platelets (3.6×10^8/ml) were preincubated for 3 min in the presence or absence of various inhibitors of selected signaling events including manumycin A (3 μM), SCH79797 (3 and 9 μM), PD98059 (20 μM), SB203580 (10 μM), LY294002 (25 μM), SP600125 (10 μM), or aristolochic acid (150 and 300 μM) before the addition of collagen (1 μg/ml), thrombin (0.6 U/ml), or amyloid-β (2 and 10 μM). Six minutes after the addition of an agonist, EDTA (2 mM) and indomethacin (50 μM) were added to the reaction suspensions. The thromboxane B_2 (TxB_2) levels in the supernatant were measured using an EIA kit according to the manufacturer's protocol.

2.5. Immunoblotting

Washed platelets (1.2×10^9/ml) were stimulated with amyloid-β or other agonists for the appropriate times, the reaction was stopped by the addition of EDTA (10 mM), and the suspensions were centrifuged and immediately re-suspended in lysis buffer. Collected lysates were centrifuged and the supernatants were separated by SDS-PAGE (12%); the proteins were electrotransferred onto a Hybond-P PVDF membrane by semidry transfer (Bio-Rad, Hercules, CA). Blots were blocked with TBST (10 mM Tris-base, 100 mM NaCl, and 0.01% Tween 20) containing 5% BSA for 1 h and then probed with primary antibody anti-p-p38 MAPK, anti-p38 MAPK, anti-p-ERKs (p42/44), anti-ERKs (p42/44), anti-p-JNK1, anti-JNK1, anti-p-Akt, or anti-Akt (diluted 1:1000 in TBST) for 2 h. Membranes were washed and then incubated with horseradish peroxidase-linked anti-mouse IgG or anti-rabbit IgG (diluted 1:3000 in TBST). Immunoreactive bands were detected by chemiluminescence using the ECL-enhanced chemiluminescence system (Amersham). For quantitative analysis of the extent of protein expression based on immunoblotting, bar graphs were created to depict the ratios of the optical density of reactive bands derived from densitometry using Bio-1D version 99 image software relative to that of control bands.

2.6. Ras activation assay

The Ras activation assay was carried out according to the instructions of the manufacturer (Upstate Biotech., Temecula, CA). In brief, washed platelets (1.2×10^9/ml) were stimulated with Aβ (10 μM), the reaction mixture was centrifuged and re-suspended in lysis buffer. Aliquots of lysates were set aside to allow quantification of total Ras by immunoblotting. The remaining lysates were incubated with beads coated with a fusion protein (GST-Raf1-RBD) consisting of GST fused to the Ras binding domain of Raf-1. Beads were washed with PBS, and bound protein was eluted with 2×Laemmli reducing sample buffer. Samples were separated by SDS-PAGE (12%); the proteins were electrotransferred for immunoblotting using horseradish peroxidase-linked anti-mouse IgG (diluted 1: 3000 in TBST) as described above.

2.7. Statistical analysis

The experimental results are expressed as mean ± S.E.M. with the number of experiments indicated. Difference among groups was assessed by the method of analysis of variance (ANOVA). If a significant difference among the group means was noted, difference between two groups was assessed using the Newman–Keuls method. A *P* value less than 0.05 was considered statistically significant.

3. Results

3.1. Effect of amyloid-β on platelet aggregation and $[Ca^{+2}]i$ mobilization

In preliminary studies, amyloid-β_{1-40} and amyloid-β_{25-35} peptides showed equal potencies in inducing platelet activation (data not shown). Subsequently all of the studies were then conducted using amyloid-β_{25-35} to explore the mechanisms of platelet activation. Amyloid-β (0.5–2 μM) concentration-dependently potentiated platelet aggregation induced by collagen (0.5 μg/ml) (Fig. 1A) and ADP (4 μM) in washed platelets (Fig. 1B) as well as platelet-rich plasma (data not shown). At these concentrations (0.5–2 μM), Aβ was not as effective in potentiating arachidonic acid

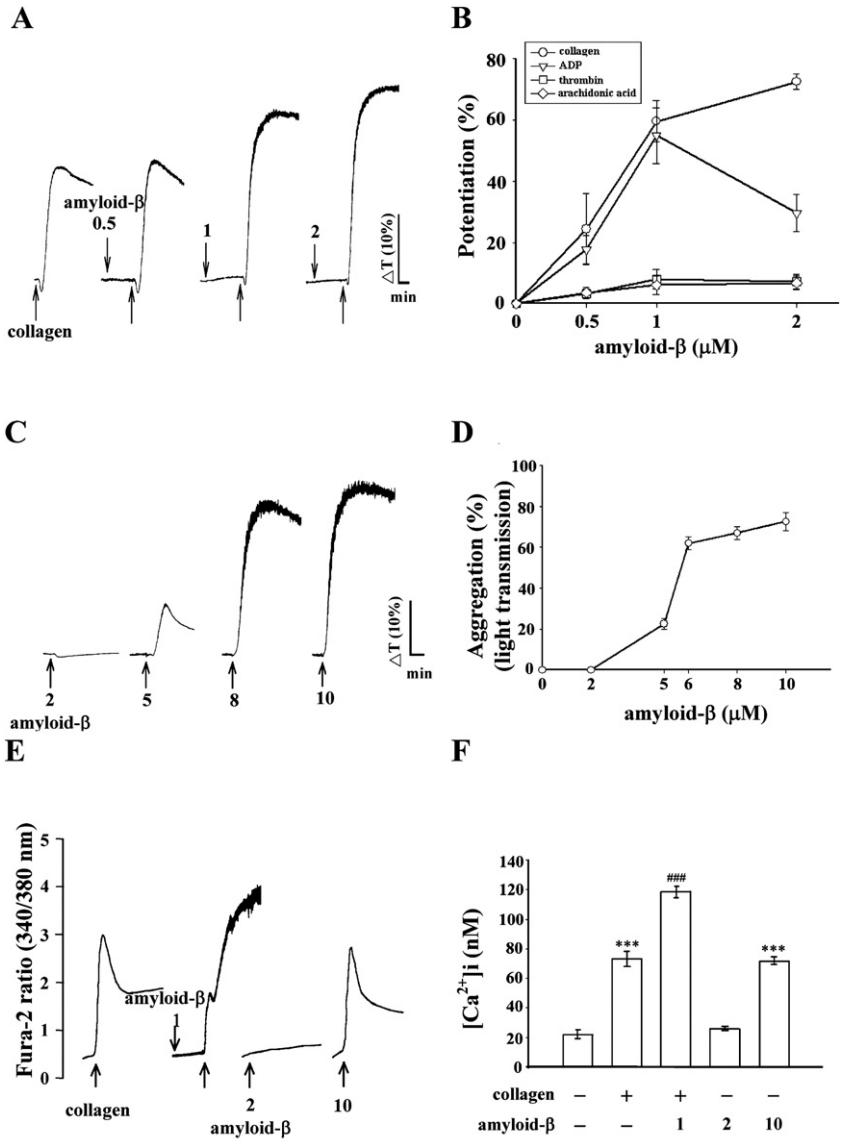

Fig. 1. Effects of amyloid-β on platelet aggregation and $[Ca^{+2}]i$ mobilization in washed human platelets. Platelets were preincubated with amyloid-β (0.5 – 10 μM) with (A, B, E, F) or without (C, D) agonists (collagen 0.5 μg/ml, ○; ADP 4 μM, ▽; thrombin 0.01 U/ml, □; or arachidonic acid 40 μM, ◇) to trigger platelet aggregation (A, B) as well as $[Ca^{+2}]i$ mobilization (E, F) in washed platelets. Data in panel B are presented as percent potentiation by amyloid-β among 4 individual agonists; data in panel D are presented as percentage aggregation induced by amyloid-β based on the extent of light transmission. Data in panels B, D and F are presented as mean ± S.E.M. ($n=4$). $^{***}P<0.001$ as compared with the control group; $^{\#\#\#}P<0.001$ as compared with the collagen group.

(40 μM)- or thrombin (0.01 U/ml)-induced platelet aggregation (Fig. 1B). At higher concentrations (2 – 10 μM), amyloid-β directly triggered platelet aggregation, with a maximal response reached at 8 – 10 μM (Fig. 1C and D). Collagen-induced platelet aggregation was accompanied by an increase in $[Ca^{+2}]i$. This collagen effect was potentiated by amyloid-β (1 μM) (Fig. 1E). At a higher concentration (5–10 μM), amyloid-β itself activated calcium influx in the absence of an agonist (Fig. 1E and F).

3.2. Effects of amyloid-β on MAPK activation

To further investigate the mechanism of amyloid-β-induced platelet activation, we surveyed the major signaling cascades including those involving JNK1, p38 MAPK, and ERK2. Immunoblotting revealed that amyloid-β (10 μM) induced time-dependent phosphorylation of JNK1, p38 MAPK, and ERK2 (Fig. 2A–C), starting as early as 0.5 min, peaking at 2–3 min and returning to basal levels 30 min after exposure. Thrombin (0.6 U/ml) and collagen (1 μg/ml) also activated JNK1 (Fig. 2A), p38 MAPK, and ERK2 (data not shown). In platelets, a likely cellular event downstream of JNK1, p38 MAPK, and ERK2 is the activation of thromboxane A_2 (TxA_2) synthesis. Amyloid-β concentration-dependently increased the formation of TxB_2, a stable metabolite of TxA_2 (control, 1.1 ± 0.7 ng/ml; 2 μM, 5.3 ± 2.8 ng/ml; 10 μM, 42.1 ± 6.8 ng/ml, $n=5$). TxB_2 formation was markedly inhibited by SCH79797, a proteinase-activated receptor 1 (PAR1) antagonist; manumycin A, a Ras inhibitor; SB203580, a p38 MAPK inhibitor; LY294002, a phosphoinositide 3-kinase (PI3-kinase) inhibitor; and aristolochic acid, a cytosolic phospholipase A_2 ($cPLA_2$) inhibitor; but not by PD98059, an ERK inhibitor, or SP600125, a JNK inhibitor (Fig. 2D). These results indicate that neither JNK1 nor ERK2 phosphorylation was involved in amyloid-β-induced TxB_2 formation. TxA_2 formation is necessary for platelet aggregation. p38 MAPK appears to provide a signal necessary for TxA_2 formation caused by amyloid-β Subsequent studies were directed at signaling events relevant to p38 MAPK phosphorylation.

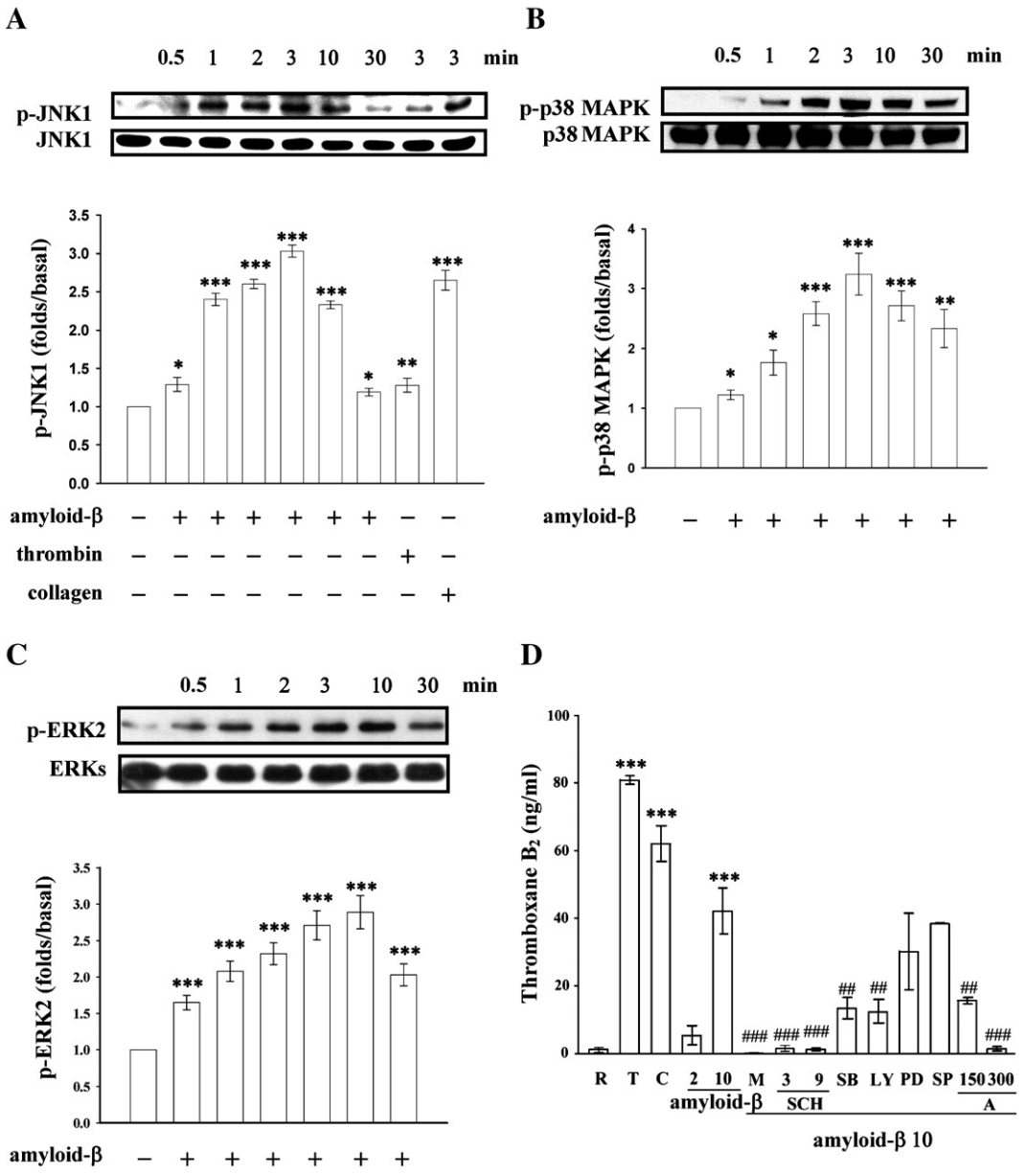

Fig. 2. Amyloid-β effects on (A) JNK1, (B) p38 MAPK, and (C) ERK2 phosphorylation or (D) thromboxane B_2 formation in washed platelets. Washed platelets were stimulated by amyloid-β (2 or 10 μM), thrombin (0.6 U/ml), or collagen (1 μg/ml) for 0.5–30 min and the extent of JNK1, p38 MAPK, and ERK2 phosphorylation were assessed by immunoblotting. For TxB_2 assay, washed platelets were preincubated with manumycin A (M, 3 μM), SCH79797 (SCH, 3 or 9 μM), SB203580 (SB, 10 μM), LY294002 (LY, 25 μM), PD98059 (PD, 20 μM), SP600125 (SP, 10 μM), and aristolochic acid (A, 150 and 300 μM), followed by the addition of Aβ (10 μM), thrombin (T, 0.6 U/ml), or collagen (C, 1 μg/ml). $^{*}P<0.05$, $^{**}P<0.01$, and $^{***}P<0.001$ in comparison with the resting group (R) ($n=4-5$); $^{\#\#}P<0.01$ and $^{\#\#\#}P<0.001$ as compared with the group treated with amyloid-β (10 μM) alone ($n=4$).

3.3. Amyloid-β activation of p38 MAPK and Akt phosphorylation in washed platelets

We first explored whether p38 MAPK is pivotal in amyloid-β-induced platelet aggregation. The effect of SB203580, a p38 MAPK inhibitor, was tested. SB203580, at a concentration of 10 μM nearly abolished amyloid-β (10 μM)-induced platelet aggregation, whereas PD98059 (20 μM, an ERK inhibitor) and SP600125 (10 μM, a JNK inhibitor) had no significant effects (Fig. 3A). To further establish the role of p38 MAPK phosphorylation in amyloid-β activation of platelets, we tested inhibitors on signaling events upstream of p38 MAPK phosphorylation. Activation of the p38 MAKP pathway following its phosphorylation has been shown to involve a number of upstream kinases including PI3-kinase and Akt. Inhibitors of PI3-kinase (LY294002) and Akt (Akt-I) significantly diminished amyloid-β-induced p38 MAPK phosphorylation without changing the amount of total p38 MAPK (Fig. 3B), indicating that PI3-kinase and Akt are upstream regulators of p38 MAPK phosphorylation in amyloid-β activation of platelets.

The PI3-kinase-Akt-p38 MAPK pathway has been well established in other cellular activation mechanisms (Zhang et al., 2005). To further establish that this cascade is in operation in amyloid-β activation of platelets, we tested the effects of LY294002, an inhibitor of PI3-kinase and Akt-I, an inhibitor of Akt on amyloid-β-induced platelet aggregation. Both inhibitors showed the expected actions in blocking platelet aggregation triggered by amyloid-β (Fig. 3C), supporting the pivotal role of the PI3-kinase-Akt-p38 MAPK cascade in amyloid-β-induced platelet aggregation. To determine the kinetics of Akt phosphorylation stimulated by amyloid-β, Ser^{473} phosphorylation was monitored over a period of 0.5–30 min. Fig. 3D shows that a rapid increase in Akt phosphorylation in response to amyloid-β (10 μM) was detectable as early as 0.5 min, peaked at about 1 min, and

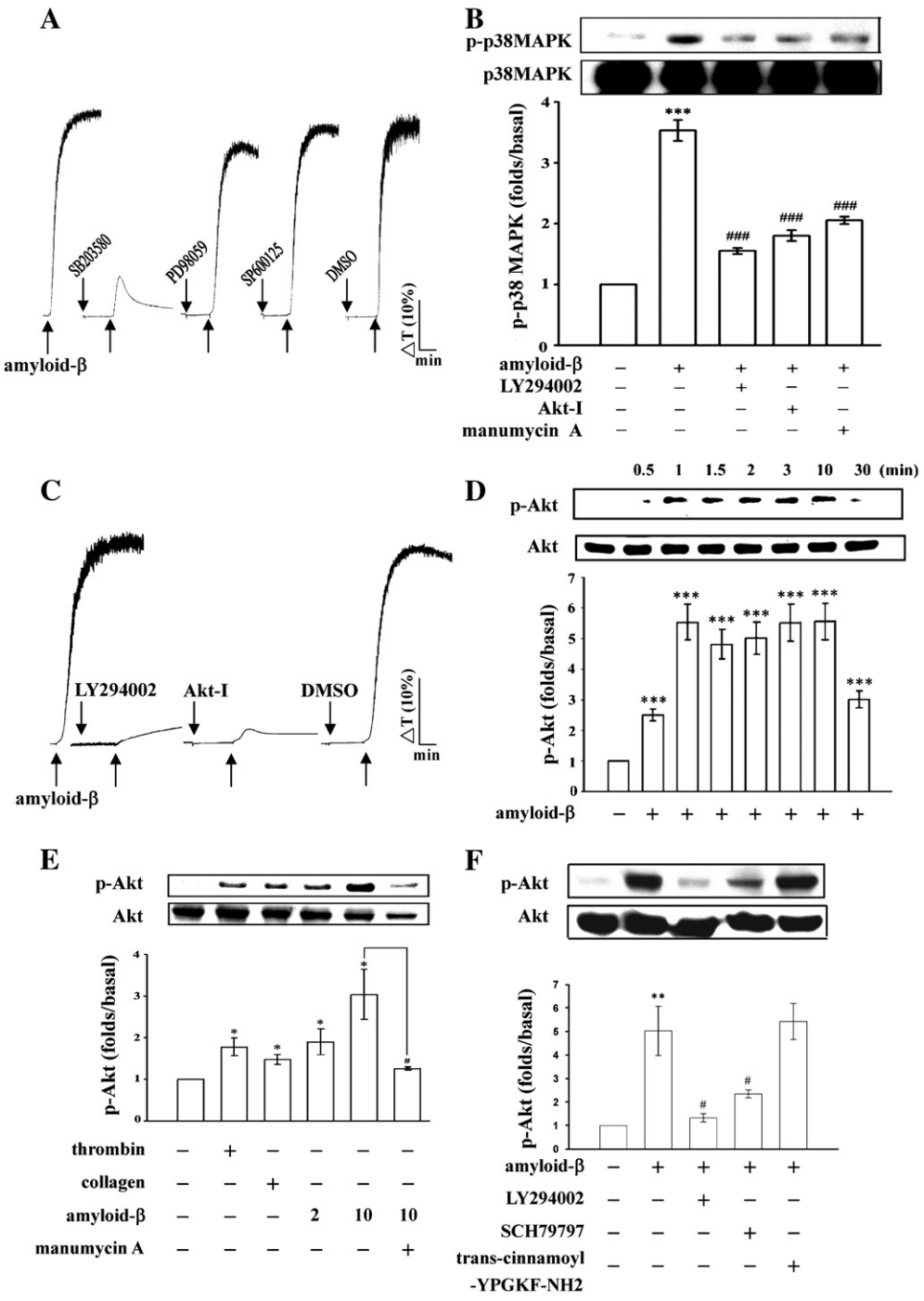

Fig. 3. Amyloid-β effects on p38 MAPK and Akt phosphorylation in washed platelets. Platelets were pretreated with SB203580 (10 μM), PD98059 (20 μM), SP600125 (10 μM) or LY294002 (25 μM), Akt-I (2 μM), or manumycin A (3 μM), followed by the addition of amyloid-β (10 μM). (A) The effects of SB 203580, PD98059, and SP600125 on amyloid-β-induced platelet aggregation. (B) Effects of LY294002 (25 μM), Akt-I (2 μM), or manumycin A (3 μM) on amyloid-β (10 μM) activation of p38 MAPK phosphorylation. (C) The effect of LY294002 (25 μM), or Akt-I (2 μM), inhibitor of Akt or p38 MAPK phosphorylation, on amyloid-β-induced platelet aggregation. (D) The time course of amyloid-β activation of Akt phosphorylation. (E) Manumycin A (3 μM) effects on amyloid-β activation of Akt phosphorylation. Thrombin (0.6 U/ml) and collagen (1 μg/ml) served as the positive controls. (F) The effects of LY294002 (25 μM), SCH79797 (9 μM) or *trans*-cinnamoyl-YPGKF-NH2 (400 μM) on amyloid-β activation of Akt phosphorylation. $^{*}P<0.05$, $^{**}P<0.01$, and $^{***}P<0.001$ in comparison with the resting group ($n=4$); $^{\#}P<0.05$ and $^{\#\#\#}P<0.001$ as compared with the group treated with amyloid-β alone ($n=4$).

remained stable after 30 min of stimulation. Thrombin (0.6 U/ml), collagen (1 μg/ml), and amyloid-β (2 and 10 μM), all induced an increase in Akt phosphorylation (Fig. 3E and F) with amyloid-β exhibiting the most pronounced concentration-dependent effect. Pretreatment with manumycin A, a Ras inhibitor (3 μM) (Fig. 3E) or LY294002, a PI3-kinase inhibitor; (25 μM) (Fig. 3F) markedly inhibited Akt phosphorylation, indicating that Ras and PI3-kinase are upstream regulators of amyloid-β-induced Akt phosphorylation. Upstream of the Ras-PI3-kinase-Akt-p38 MAPK cascade is the proteinase-activated receptor (PAR). As described earlier (Fig. 2D), amyloid-β-induced TxB_2 formation was significantly inhibited by SCH79797, a PAR1 antagonist. In Fig. 3F, SCH79797 (9 μM) but not *trans*-cinnamoyl-YPGKF-NH2 (400 μM), a PAR4 antagonist, abolished Akt phosphorylation induced by amyloid-β. This finding raises the possibility that PAR1 may be integral to the Ras-PI3-kinase-Akt-p38 MAPK cascade in amyloid-β activation of platelets.

3.4. Effect of PAR1 and PAR4 antagonists on amyloid-β-induced platelet activation

To further assess the roles of PAR1 and PAR4 in amyloid-β-induced platelet activation, SCH79797, a PAR1 antagonist, and *trans*-cinnamoyl-YPGKF-NH2, a PAR4 antagonist, were further tested. SCH79797 (3 and 9 μM) but not *trans*-cinnamoyl-YPGKF-NH2 (400 μM) concentration-dependently inhibited amyloid-β (10 μM) activation of platelet aggregation (Fig. 4A and B). SCH79797 and *trans*-cinnamoyl-YPGKF-NH2 were also tested the possible roles of PAR1 and PAR4 in the Ras-PI3-kinase-Akt-p38 MAPK cascade in amyloid-β activation of platelets. Amyloid-β (10 μM)-induced p38 MAPK phosphorylation was markedly inhibited by SCH79797 (3 and 9 μM) (Fig. 4C), but not by *trans*-cinnamoyl-YPGKF-NH2 (400 μM), a PAR4 antagonist (data not shown). SCH79797 was less effective in thrombin (0.6 U/ml)-induced p38 MAPK phosphorylation. To further confirm the role of PAR1 in the Ras-PI3-kinase-Akt-p38 MAPK cascade, we applied a Ras activity assay to study the effect of SCH79797, a PAR1 antagonist. Amyloid-β (10 μM) induced an increase in Ras activation (Ras-GTP), which was markedly inhibited by SCH79797 (9 μM), but not by *trans*-cinnamoyl-YPGKF-NH2 (400 μM), a PAR4 antagonist (Fig. 4D). The effect of SCH79797 on Ras activity, Akt and p38 MAPK phosphorylation are consistent with the contention that the PAR1-Ras-PI3-kinase-Akt-p38 MAPK-cPLA$_2$-TxA$_2$ cascade is activated in amyloid-β-induced platelet aggregation.

4. Discussion

Results obtained from the present study demonstrate for the first time the activation of the PAR1-Ras-PI3-kinase-Akt-p38 MAPK-cPLA$_2$-TxA$_2$ cascades in amyloid-β-induced platelet activation. Amyloid-β's actions on platelets were concentration dependent. At lower concentrations (0.5–2 μM), amyloid-β potentiated agonist-induced platelet aggregation, whereas at higher concentrations (2–10 μM), amyloid-β itself directly activated the aggregatory responses. It is conceivable that the amyloid-β concentration may be high at the site of vascular injury where platelet activation can lead to amyloid-β secretion into the extracellular space, creating a vicious cycle of platelet aggregation. It is

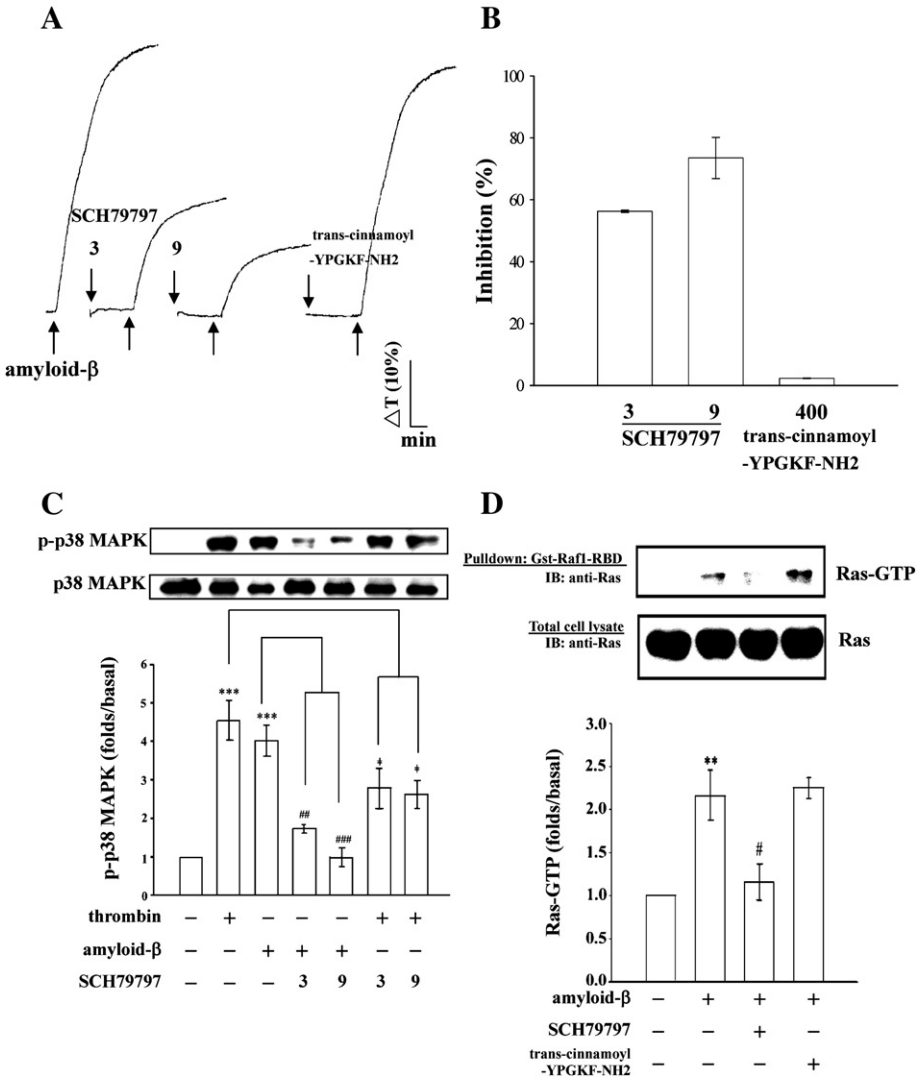

Fig. 4. Effects of SCH79797 and *trans*-cinnamoyl-YPGKF-NH2 on platelet activation stimulated by amyloid-β. Platelets were pretreated with SCH79797 (3 and 9 μM) or *trans*-cinnamoyl-YPGKF-NH2 (400 μM), followed by the addition of amyloid-β (10 μM) to trigger platelet aggregation (A, B) or p38 MAPK phosphorylation (C). Note SCH79797 but not *trans*-cinnamoyl-YPGKF-NH2, was effective in inhibiting amyloid-β-induced platelet aggregation and p38 MAPK phosphorylation. SCH79797 was less effective in inhibiting p38 MAPK phosphorylation induced by thrombin (0.6 U/ml) (C). SCH79797 but not *trans*-cinnamoyl-YPGKF-NH2, inhibited amyloid-β activation of Ras activity using an assay based on pulling down active GTP-loaded Ras with a GST fusion protein containing the Ras binding domain of Raf-1 (GST-Raf1-RBD) as described in "Materials and methods" (D). $^{**}P<0.01$ and $^{***}P<0.001$ as compared with the resting group ($n=4$); $^{\#}P<0.05$, $^{\#\#}P<0.01$, and $^{\#\#\#}P<0.001$ as compared with the amyloid-β-treated group ($n=4$); $^{\ddagger}P<0.05$ as compared with the thrombin-treated group ($n=4$).

now well established that the aggregated state of amyloid-β is closely linked to their toxicity. In this study, we found that amyloid-β_{25-35} (20 μM) or amyloid-β_{1-40} (20 μM) incubated with platelets for 10 min did not significantly increase lactate dehydrogenase activity compared with resting platelets (data not shown), indicating that amyloid-β did not affect platelet permeabilization or induce platelet cytolysis under this concentration, clearly disproving the cytotoxic effect of amyloid-β on platelets in this study.

MAPKs family consists of three major subgroups. The ERKs are involved in proliferation, adhesion, and cell progression (Bugaud et al., 1999). p38 MAPK and JNKs which includes the 46-kDa JNK1 and 55-kDa JNK2 isoforms, are involved in death signaling processes (Bugaud et al., 1999). In platelets, three MAPKs, namely ERKs, JNK1, and p38 MAPK, have been identified (Bugaud et al., 1999). The ERK (p44 ERK1 and p42 ERK2) cascade is activated by thrombin or collagen, via the MEK 1/2 (Rosado and Sage, 2002). JNK1 is present and active in platelets and has a similar regulatory role as ERK2 (Bugaud et al., 1999). p38 MAPK provides a crucial signal which is necessary for the aggregation caused by collagen or thrombin (Saklatvala et al., 1996). In the present study, amyloid-β time-dependently triggered p38 MAPK, JNK1, and ERK2 phosphorylation. In addition, amyloid-β-induced TxA_2 formation was inhibited by a p38 MAPK inhibitor, but not by JNK or ERK inhibitors (Fig. 2D). This is consistent with a previous report which found that flurbiprofen, a cycloxygenase I inhibitor, had no effect on thrombin-induced JNK1 or ERK2 phosphorylation, suggesting that TxA_2 formation is not involved in JNK1 and ERK2 activation in human platelets (Bugaud et al., 1999). The roles of JNK1 and ERK2 in platelet activation are unclear. They may serve as suppressors in $\alpha_{IIb}\beta_3$ activation or as negative regulators of platelet activation (Hughes et al., 1997). p38 MAPK appears to be involved in the TxA_2-dependent platelet aggregation pathway. Among the numerous downstream targets of p38 MAPK, the most physiologically relevant one in platelets is $cPLA_2$ which catalyses the release of arachidonic acid for TxA_2 synthesis (Coulon et al., 2003). Results from the present study also provide supporting evidence that $cPLA_2$ activation downstream of p38 MAPK is a crucial step in amyloid-β-induced platelet aggregation (Fig. 5).

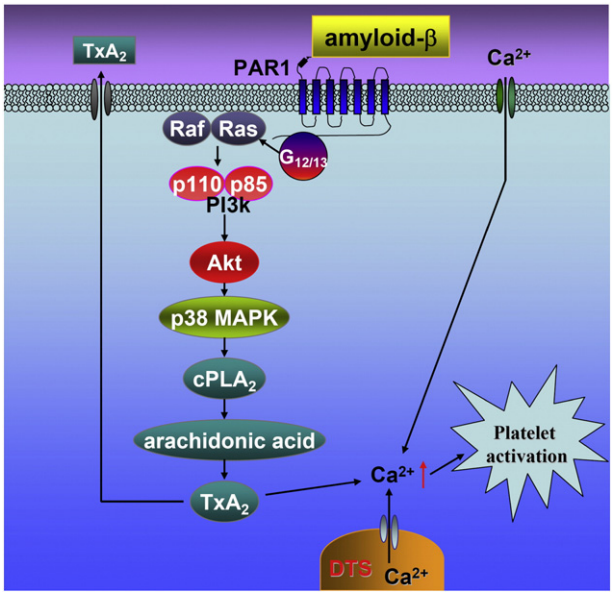

Fig. 5. The hypothesis of signal transductions of amyloid-β-induced platelet activation. Amyloid-β binds to G protein (i.e., $G_{12/13}$)-coupled proteinase-activated receptor 1 (PAR1), and then activates kinases (i.e., Ras). Ras binds to Raf at the membrane and is phosphorylated, which subsequently activates the PI3-kinase-Akt cascade, which is followed by activation of p38 MAPK. p38 MAPK can activate cytosolic phospholipase A_2 ($cPLA_2$), which catalyses arachidonic acid release to produce thromboxane A_2 (TxA_2) formation.

Stimulation of platelets with various agonists results in Akt activation. Although it is known that Akt functions as one of several downstream effectors of PI3-kinase (Franke et al., 1995), the molecular mechanism underlying Akt activation in platelets is not well established. Thus, we also investigated the signaling events involving Akt activation mediated by amyloid-β in platelets. In this study, both manumycin A, a Ras inhibitor, and LY294002, a PI3-kinase inhibitor, inhibited amyloid-β-induced Akt phosphorylation, consistent with a causal role of Ras in the activation of the PI3-kinase-Akt pathway (McCormick and Wittinghofer, 1996). Inhibitors of Ras, PI3-kinase, and Akt also inhibited p38 MAPK phosphorylation induced by amyloid-β. It is well-known that Ras cascade activation is involved in the activation of MAPKs (Hughes et al., 1997). The interaction of Ras with Raf is the most thoroughly characterized of these interactions. Raf regulates MEK, which in turn activates MAPKs including p38 MAPK. Results from the present study are consistent with the contention that the Ras-PI3-kinase-Akt-p38 MAPK-$cPLA_2$-TxA_2 pathway plays a pivotal role in amyloid-β-induced platelet activation (Fig. 5).

Platelet activation has also been shown to involve a family of $G_{12/13}$-coupled proteinase-activated receptors (PARs). In human platelets, PARs are divided into two major receptors: a high-affinity PAR1 and a low-affinity PAR4 (Kahn et al., 1998). In this study, SCH79797, a PAR1 antagonist, but not *trans*-cinnamoyl-YPGKF-NH2, a PAR4 antagonist, inhibited amyloid-β-induced increase in Ras activity and the phosphorylation of Akt, and p38 MAPK as well as amyloid-β-induced platelet aggregation. These results together suggest the presence of G protein-coupled PAR1 receptor mechanism which is upstream of the Ras-PI3-kinase-Akt-p38 MAPK-$cPLA_2$-TxA_2 cascade amyloid-β-induced platelet aggregation (Fig. 5). Understanding the cellular signaling processes that underlie amyloid-β activation of platelets may contribute our knowledge of cerebrovascular degeneration involving age-dependent vascular deposition of amyloid-β in the brain, particularly cerebral amyloid angiopathy and aid in future development of preventive or therapeutic strategies to slow down the development of cerebral amyloid angiopathy.

Acknowledgements

This work was supported by grants from the National Science Council of Taiwan (NSC92-2321-B-038-001, 93-2321-B-038-001, and 94-2321-B-038-001) and Ministry of Education Topnotch Stroke Research Center, Taiwan. The authors declare no competing financial interests.

References

Bugaud, F., Nadal-Wollbold, F., Levy-Toledano, S., Rosa, J.P., Bryckaert, M., 1999. Regulation of c-*jun*-NH2 terminal kinase and extracellular-signal regulated kinase in human platelets. Blood 94, 3800–3805.

Chen, M., Inestrosa, N.C., Ross, G.S., Fernandez, H.L., 1995. Platelets are the primary source of amyloid β-peptide in human blood. Biochem. Biophys. Res. Commun. 213, 96–103.

Coulon, L., Calzada, C., Moulin, P., Vericel, E., Lagarde, M., 2003. Activation of p38 mitogen-activated protein kinase/cytosolic phospholipase A_2 cascade in hydroperoxide-stressed platelets. Free Radic. Biol. Med. 35, 616–625.

Franke, T.F., Yang, S.I., Chan, T.O., Datta, K., Kazlauskas, A., Morrison, D.K., Kaplan, D.R., Tsichlis, P.N., 1995. The protein kinase encoded by the Akt proto-oncogene is a target of the PDGF-activated phosphatidylinositol 3-kinase. Cell 81, 727–736.

Fryer, J.D., Simmons, K., Parsadanian, M., Bales, K.R., Paul, S.M., Sullivan, P.M., Holtzman, D.M., 2005. Human apolipoprotein E4 alters the amyloid-beta 40:42 ratio and promotes the formation of cerebral amyloid angiopathy in an amyloid precursor protein transgenic model. J. Neurosci. 25, 2803–2810.

Gurol, M.E., Irizarry, M.C., Smith, E.E., Raju, S., Diaz-Arrastia, R., Bottiglieri, T., Rosand, J., Growdon, J.H., Greenberg, S.M., 2006. Plasma beta-amyloid and white matter lesions in AD, MCI, and cerebral amyloid angiopathy. Neurology 66, 23–29.

Herczenik, E., Bouma, B., Korporaal, S.J.A., Strangi, R., Zeng, Q., Gros, P., Van Eck, M., Van Berkel, T.J.C., Gebbink, M.F.B.G., Akkerman, J.N., 2007. Activation of human platelets by misfolded protein. Arterioscler. Thromb. Vasc. Biol. 27, 1657–1665.

Herzig, M.C., Winkler, D.T., Burgermeister, P., Pfeifer, M., Kohler, E., Schmidt, S.D., Danner, S., Abramowski, D., Sturchler-Pierrat, C., Burki, K., van Duinen, S.G., Maat-Schieman, M.L., Staufenbiel, M., Mathews, P.M., Jucker, M., 2004. Abeta is targeted to the vasculature in a mouse model of hereditary cerebral hemorrhage with amyloidosis. Nat. Neurosci. 7, 954–960.

Hsiao, G., Lin, K.H., Chang, Y., Chen, T.L., Tzu, N.H., Chou, D.S., Sheu, J.R., 2005. Protective mechanisms of inosine in platelet activation and cerebral ischemic damage. Arterioscler. Thromb. Vasc. Biol. 25, 1998–2004.

Hsiao, G., Lee, J.J., Lin, K.H., Shen, C.H., Fong, T.H., Chou, D.S., Sheu, J.R., 2007. Characterization of a novel and potent collagen antagonist, caffeic acid phenethyl ester, in human platelets: in vitro and in vivo studies. Cardiovasc. Res. 75, 782–792.

Hsu, M.J., Hsu, C.Y., Chen, B.C., Chen, M.C., Ou, G., Lin, C.H., 2007. Apoptosis signal-regulating kinase 1 in amyloid beta peptide-induced cerebral endothelial cell apoptosis. J. Neurosci. 27, 5719–5729.

Hughes, P.E., Renshaw, M.W., Pfaff, M., Forsyth, J., Keivens, V.M., Schwartz, M.A., Ginsberg, M.H., 1997. Suppression of integrin activation: a novel function of a Ras/Raf-initiated MAP kinase pathway. Cell 88, 521–530.

Kahn, M.L., Zheng, Y.W., Huang, W., Bigornia, V., Zeng, D., Moff, S., Farese Jr., R.V., Tam, C., Coughlin, S.R., 1998. A dual thrombin receptor system for platelet activation. Nature 394, 690–694.

Li, Q.X., Berndt, M.C., Bush, A.I., Rumble, B., Mackenzie, I., Friedhuber, A., Beyreuther, K., Masters, C.L., 1994. Membrane-associated forms of the beta A4 amyloid protein precursor of Alzheimer's disease in human platelets and brain: surface expression on the activated human platelet. Blood 84, 133–142.

Mackic, J.B., Bading, J., Ghiso, J., Walker, L., Wisniewski, T., Frangione, B., Zlokovic, B.V., 2002. Circulating amyloid-beta peptide crosses the blood-brain barrier in aged monkeys and contributes to Alzheimer's disease lesions. Vascul. Pharmacol. 38, 303–313.

McCormick, F., Wittinghofer, A., 1996. Interactions between Ras proteins and their effectors. Curr. Opin. Biotechnol. 7, 449–456.

Rosado, J.A., Sage, S.O., 2002. The ERK cascade, a new pathway involved in the activation of store-mediated calcium entry in human platelets. Trends Cardiovasc. Med. 12, 229–234.

Saklatvala, J., Rawlinson, L., Waller, R.J., Sarsfield, S., Lee, J.C., Morton, L.F., Barnes, M.J., Farndale, R.W., 1996. Role for p38 mitogen-activated protein kinase in platelet aggregation caused by collagen or a thromboxane analogue. J. Biol. Chem. 271, 6586–6589.

Sheu, J.R., Hung, W.C., Wu, C.H., Ma, M.C., Kan, Y.C., Lin, C.H., Lin, M.S., Luk, H.N., Yen, M.H., 1999. Reduction in lipopolysaccharide-induced thrombocytopenia by triflavin in a rat model of septicemia. Circulation 99, 3056–3062.

Skovronsky, D.M., Lee, V.M., Pratico, D., 2001. Amyloid precursor protein and amyloid beta peptide in human platelets. Role of cyclooxygenase and protein kinase. C. J. Biol. Chem. 276, 17036–17043.

Smith, C.C., 1997. Stimulated release of the β-amyloid protein of Alzheimer's disease by normal human platelets. Neurosci. Lett. 235, 157–159.

Tedgui, A., Mallat, Z., 2002. Platelets in atherosclerosis: a new role for beta-amyloid peptide beyond Alzheimer's disease. Circ. Res. 90, 1145–1146.

van Dijk, E.J., Prins, N.D., Vermeer, S.E., Hofman, A., van Duijn, C.M., Koudstaal, P.J., Breteler, M.M., 2004. Plasma amyloid beta, apolipoprotein E, lacunar infarcts, and white matter lesions. Ann. Neurol. 55, 570–575.

Wisniewski, T., Ghiso, J., Frangione, B., 1997. Biology of β-amyloid in Alzheimer's disease. Neurobiol. Dis. 4, 313–328.

Zhang, X., Shan, P., Alam, J., Fu, X.Y., Lee, P.J., 2005. Carbon monoxide differentially modulates STAT1 and STAT3 and inhibits apoptosis via a phosphatidylinositol 3-kinase/Akt and p38 Kinase-dependent STAT3 pathway during anoxia-reoxygenation injury. J. Biol. Chem. 280, 8714–8721.

Zhang-Nunes, S.X., Maat-Schieman, M.L., van Duinen, S.G., Roos, R.A., Frosch, M.P., Greenberg, S.M., 2006. The cerebral beta-amyloid angiopathies: hereditary and sporadic. Brain Pathol. 16, 30–39.